

Cold Spray metal powder deposition with 9 %Cr-steel applied for the HCPB First Wall fabrication: Proof of concept and options for ODS steel processing

Heiko Neuberger^{a,*}, Francisco Hernandez^a, Michael Rieth^b, Carsten Bonnekoh^b, Ludek Stratil^c, Ivo Dlouhy^c, Petr Dymacek^c, Oliver Müller^d, Lucas Adler^d, Ulrich Kunert^e

^a Karlsruhe Institute of Technology (KIT), Institute of Neutron Physics and Reactor Technology (INR), Germany

^b Karlsruhe Institute of Technology (KIT), Institute of Applied Materials (IAM-AWP), Germany

^c Institute of Physics of Materials ASCR, Brno, Czech Republic

^d Hermle Maschinenbau GmbH, Ottobrunn, Germany

^e PHA Werkstofftechnik, Lüdinghausen, Germany

ARTICLE INFO

Keywords:

First Wall
Additive Manufacturing
Cold Spray deposition
Oxide dispersion strengthened materials

ABSTRACT

At the KIT a hybrid manufacturing concept for nuclear fusion First Walls is developed combining aspects of conventional and Additive Manufacturing (AM) technologies. The state of the art for ITER does not cover all specifications of a DEMO relevant First Wall. Thus, additional R&D-work has been initiated in terms of manufacturing. The AM technology basis used in the presented process combination is Cold Spray metal powder deposition applied in alternation with machining including the feature of filling grooves temporarily with a water-soluble granulate for creation of closed channels and cavities. Thus, the technology provides the option to manufacture shells with a thin gas tight membrane on top of previously machined structures. This membrane is used as pressure seal and makes the joining of shells by Hot Isostatic Pressing (HIP) into one monolithic body possible. This paper describes the manufacturing process and recalls differences and common aspects with regard to conventional concepts of First Wall manufacturing. The achievement of Technology Readiness Level TRL 3 by mechanical qualification and comparison of the results to other HIP joint experiments is also demonstrated. Finally, an outlook is given concerning integration options of the technology into manufacturing of shells with cooling channel structures using Oxide Dispersion Strengthened (ODS) materials.

Introduction

A variety of approaches have been launched worldwide and within Europe during the recent decade and even before in order to develop manufacturing strategies for ITER relevant Test Blanket Module (TBM) components. In KIT this topic was addressed in 2010 aiming on realization of TBM sub components in industrial collaborations [1–3]. However, the main attention was and still is on development of manufacturing strategies for the main demanding component, the First Wall. The First Wall is the plasma facing front shell of a Blanket device in a fusion reactor, thus it shall be fully equipped with a dense pattern of cooling channels. The present state of the art in terms of nuclear fusion First Wall manufacturing is presently well reflected by ITER where a concept for manufacturing of the First Wall basing on conventional technologies (machining, Laser-welding and finally diffusion welding) was selected [4,5].

In terms of DEMO, the next development stage of tokamak fusion reactors, the manufacturing technologies for ITER First Walls however needs to be re-considered. There are significantly more demanding requirements ([6–9]) in terms of dimensions in vertical direction, the target value exceeds 10 m, which means an increase by a factor 5 compared to ITER. In terms of the geometry, the surfaces of the First Wall are no more planar, they shall be complex shaped 3D-geometries including a roof-top-shape on the plasma facing wall. For gas cooled concepts such as the Helium Cooled Pebble Bed (HCPB), another modification needs to be considered compared to the TBM since local turbulence promoters may be needed to be installed on the First Wall inner surface, [10,11]. All these aspects have a significant impact on the First Wall manufacturing concept to be developed for DEMO which may not be solved just by extrapolation of existing fabrication technology. New solution options are required.

During the 2010s the technological field of Additive Manufacturing

* Corresponding author.

E-mail address: heiko.neuberger@kit.edu (H. Neuberger).

<https://doi.org/10.1016/j.nme.2023.101427>

Received 13 January 2023; Received in revised form 8 March 2023; Accepted 26 March 2023

Available online 30 March 2023

2352-1791/© 2023 The Authors. Published by Elsevier Ltd. This is an open access article under the CC BY-NC-ND license (<http://creativecommons.org/licenses/by-nc-nd/4.0/>).

(AM) has gained significantly more visibility in industrial processes. An excellent overview on the different AM technologies (powder bed as well as direct energy deposition-based technologies) and their capabilities in terms of geometry reproduction and precision versus metal deposition rate is given in [12]. This study performed by NASA investigates AM options for liquid rocket engine combustion devices, which are, such as nuclear fusion First Wall devices, high performance heat load components with a dense pattern of cooling channels in dimensions up to 1 m and beyond. In 2015 the use of AM for fabrication of nuclear fusion reactor components has been firstly addressed in KIT and the related studies were expanded steadily until now [13–17]. Different technology concepts of AM (powder bed-based AM processes as well as direct energy deposition processes) were tested in industrial collaborations looking for the best compromise in between deposition rate, geometry reproduction capabilities, surface quality and effort in terms of licensing/material properties.

Based on the experiences gained from the various studies, starting in 2018 the development strategy has been re-aligned in order to search for combinations of AM and conventional manufacturing processes. The goal was on one hand to expand existing limits in AM, but also to find new process configurations using benefits of AM and to unite them with well-established conventional technologies [13,18–20]. The most promising technology approach found in combination of AM and conventional technologies up to now [15] is a process chain integrating the AM (direct energy deposition) process of Cold Spray metal powder deposition into the conventional First Wall manufacturing procedure proposed for ITER, e.g. [4].

Cold Spray based hybrid manufacturing: Common features shared with conventional approaches

The basic idea of the new Cold Spray metal powder deposition based fabrication process generally corresponds to the strategy already applied in conventional fabrication concepts proposed e.g. for the HCPB- or Helium Cooled Lithium Lead (HCLL) First Wall concept [2,4] consisting of three fabrication key steps (A – C, Fig. 1):

- (A) the plasma facing (external) shell is equipped on its non-plasma facing side with grooves by machining,
- (B) the grooves are sealed by a leak tight metal layer (e.g. by Laser welding of stripes) to form leak tight channels with a membrane on top with at least one opening to the external atmosphere e.g. on the face sides of the plate and finally,
- (C) joining the external shell with a second (internal) shell on top of the sealed grooves by diffusion welding (Hot Isostatic Pressing, HIP) after a circumferential weld is established by Electron Beam (EB) welding which completely surrounds the contact surface between the internal and the external shell. The HIP pressure is applied in a configuration with opened channels. Thus, the bonding pressure establishing the connection between the cover and the substrate plate with the membranes on top acts hydrostatically from outside of the part as well as from inside via the channels cavities to fully join the contact surface surrounded by an EB weld (Fig. 1, step 7).

The innovation of the new proposed hybrid technology involving AM presented in this paper lies in the sequencing and used process configuration for applying Step B, see Fig. 1, sequence of step 2 to step 6 which are explained in detail in chapter 3.

The detailed process sequence of the new Cold Spray based hybrid manufacturing process

The full Cold Spray based hybrid manufacturing process consists of a number of 9 steps: all the steps (Fig. 1) and preliminary parameters as applied in the demonstration experiment to manufacture a first

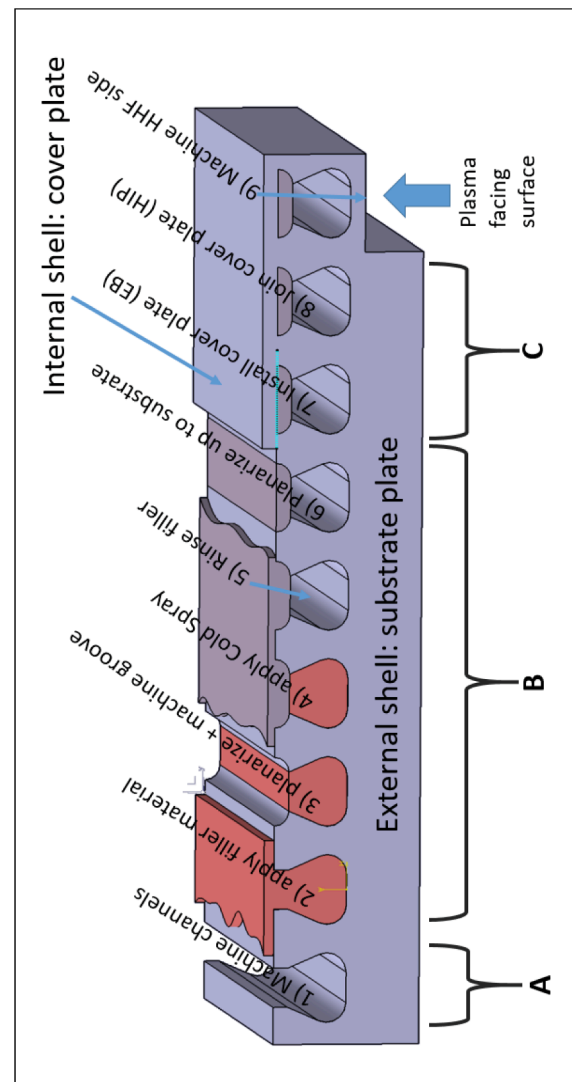


Fig. 1. Scheme of fabrication sequence indicating key steps A – C and all sub-steps 1 – 9.

demonstration part as specified in 5 are described in detail as follows:

Step 1: A heat-treated P92 plate (softening for improvement of the adhesion was applied for the first approach) has been used as substrate for the manufacturing experiment. The channels were machined using an undercut lollipop-shaped milling tool. The pear-shape of the cross section was optimized in order to maximize the contact surface in between the substrate- and cover plate for the diffusion weld on top of the channels applied at the end of the production process.

Step 2: The grooves of the plate were completely filled with the water-soluble granulate, also the integral surface of the plate was covered with granulate using the Cold Spray deposition process creating a continuous layer of the granulate. The granulate is deposited onto surfaces by the same equipment used for deposition of the metal powder (acceleration of particles in a spray gun). The Cold Spray metal powder deposition process configuration together with filling of channels with water soluble granulate applied is offered by the supplier Hermle Maschinenbau GmbH, Germany as so called Metal Powder Application (MPA).

Step 3: The whole top surface of the part was machined into a plane surface after deposition of the filler material using a face milling cutter where the cutting depth was adjusted slightly below the

surface of the initial top surface of the part. Then, additionally a groove with a depth of ~ 1 mm was machined into the surface on top of the channel using a torus cutter milling tool.

Step 4: The integral surface of the substrate plate was covered with a layer of P92 powder by MPA deposition where the previously machined grooves were completely filled with metal powder solidified due to the kinetic energy of the particles. The metal powder used in the experiment was produced by water atomization. During the deposition process, the deposited material on top of the channels was mechanically supported by the water soluble granulate filling the channel and the edges of the previously machined groove in order to gain a geometrically fully defined bottom side of the membrane.

Step 5: The filler material was rinsed by water to re-open the cavities of the channels. The deposited material remained as a membrane-like continuous leak tight layer on top of the channel in between the edges of the machined grooves on top of the channel.

Step 6: The integral surface of the part was machined into a plane surface using a face milling cutter where the cutting depth was adjusted again slightly below the surface of the initial top surface of the part to provide an oxide-free surface as preparation of the diffusion welding surface. Thus, the deposited material previously applied to fill the grooves on top of the channels remained as a membrane of ~ 1 mm thickness on top of the channels.

Step 7: On top of the membranes a cover plate was placed, tacked and installed by Electron-Beam welding. During welding the evacuation of the bonding zone for the diffusion weld in the vacuum chamber of the EB welding facility was provided. The Electron Beam weld fully surrounded and sealed the contact surface in between the cover and the substrate plate. The penetration depth of the weld was in the order of few millimeters, approximately 2 mm, since it is only needed to provide sealing function during the diffusion welding.

Step 8: The applied diffusion welding parameters 140 MPa/1050 °C/ 1.5 h (HIP with channels opened on the face sides of the demonstrator) for joining of the substrate- and cover plate included the austenitization of the material. Sufficient hold time (1.5 h) of the HIP treatment to properly establish the diffusion weld was applied. The component was directly quenched in the hot isostatic press. Then, final thermal treatment of the component tempering 760 °C/ 1.5 h was carried out to obtain desired microstructure of P92 steel tempered martensite.

Step 9: Finally, the product was machined into its final dimensions where also the Electron Beam including heat affected zone weld was fully removed.

Advantages of the Cold Spray based hybrid fabrication

In comparison to the conventional manufacturing methods discussed in 2 the Cold Spray based hybrid fabrication with the Metal Powder Application (MPA) technology of Hermle provides three advantages:

- Due to the generation of the membranes covering the grooves and sealing the HIP surface on top of the substrate plate by Cold Spray metal powder deposition (see step 8, Fig. 1) neither stripes or tubes are needed to be prepared in high precision, nor installation of sheet metal covers by fusion welding (e.g. Laser) is required. This feature is an important issue for cost reduction and to eliminate fusion welding joints from the final product.
- The adhesion of the metal powder grains during Cold Spray deposition mainly bases on kinetic energy of particles and their impact on the substrate surface. Thus, the maximum process temperature is significantly below the melting temperature of steel. This feature minimizes thermal distortion effects on the product. Since the metal powder does not melt, even the deposition of Oxide Dispersion Strengthened (ODS) metal powder material may be considered using the MPA/Cold Spray technology. Dedicated options and examples for

application of ODS materials in First Walls are described in the chapter 9.

- The share of powder metal in the final product in comparison to the amount of conventionally produced steel is in the order of 5 % due to the low thickness of the applied membrane. This is another aspect concerning cost effectivity.

Demonstration parts specifications

The fabrication specification of the first small scale mock up in plane configuration (see Fig. 2) were designed to include all the relevant manufacturing steps shown in Fig. 1.

The planar demonstration part was designed with three parallel channels with a pitch of 20 mm at a First Wall relevant cross section. The scope of the test part was to demonstrate all fabrication steps previously developed and separately qualified in out of pile experiments [15] into one continuous fabrication sequence. The requirements concerning external dimensions of the demonstration parts towards full scale Breeding Blanket First Walls (more than 10 m in main dimension and ~ 20 m² high heat flux surface) will be addressed after successful fabrication and qualification of demonstration parts using the fabrication devices presently existing in industry. The limits in terms of maximum dimension is presently ~ 0.5 m² High Heat Flux surface at the used industrial equipment. However, the dimensions limits in the process of metal powder deposition are not strictly limited due to physical or technological issues generally, the used equipment may be modified or re-configured in order to expand processing dimensions significantly.

The production experiments were (and presently still are) performed using the material P92 (1.4901) which is a 9 % Cr-steel with a comparable composition to EUROFER [21] because of the limited availability of EUROFER 97 in relevant dimensions (plates and bars for atomization to produce metal powder).

Test strategy to demonstrate proof of concept

The verification of a successful manufacturing experiment reported

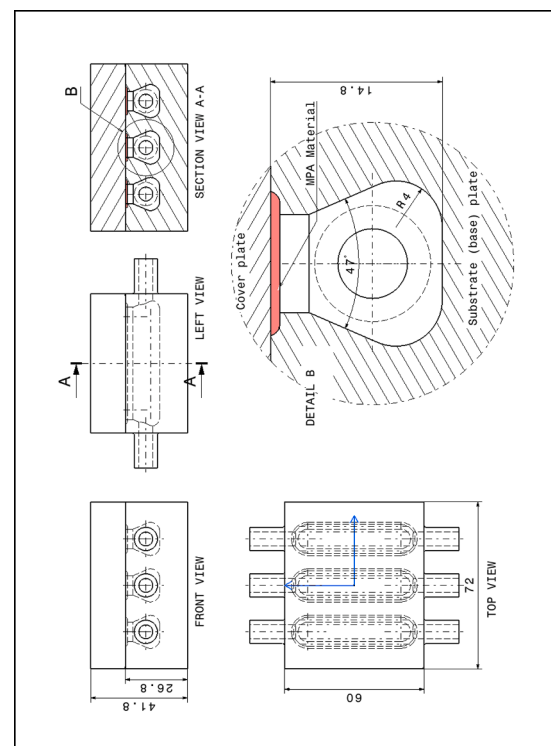


Fig. 2. Demonstration part with dimensions indicated (after fabrication step 4).

in this paper was done by quantifying the welding quality of the diffusion weld (HIP) connecting the external (substrate plate top surface opposite to the plasma side) and internal shell (non-plasma facing shell), see Fig. 1. An acceptable welding quality demonstrated the leak tightness of the membrane built from the Cold Spray deposited material. The quality of the HIP weld was quantified in several ways: by metallographic analysis as well as comparing mechanical properties to base material of the P92 steel used in the fabrication experiments. The destructive examination was performed at the Institute of Physics of Materials. The demonstration part after finishing of the fabrication sequence including machining of pressure connectors is shown in Fig. 3. The specimen extraction for the qualification of the demonstration part is shown in Fig. 4.

Methodology of the experiment

For metallography examination, several samples from selected locations of the component containing the HIP joint interface MPA layer were extracted, Fig. 4 (cutting plan of the component including metallography and mechanical specimens). The metallography analysis of the samples containing the HIP joint was performed in non-etched state to reveal any possible discontinuities at the HIP joint interface and in etched state to study the microstructures of the joint and of the joint plates. Samples in non-etched state were prepared by grinding using sandpapers of grain size from P400 to P2500, further polishing by 3 and 1 μm diamond paste and finalization by mechanical-chemical polishing by OPS suspension (Struers) for 5 min. In etched state the microstructure of samples was revealed by chemical etching in Vilella Bain for 12 s. Light microscopy (LM) and secondary electron microscopy (SEM) observation was conducted using digital microscope Olympus DSX1000 and Tescan LYRA 3 XMH FEG/SEM, respectively. Scanning electron microscopy (SEM) observation was performed using an acceleration voltage 10 kV in secondary electron mode. In total, four metallography specimens were prepared and analyzed. Hardness measurement was conducted by Vickers method using the tester Zwick Z2.5 equipped with instrumented hardness head ZHU0.2 at loading 1 kg (HV1). Hardness was measured in lines across the HIP interface with distance between the indents 0.4 mm for each sample.

Mechanical characterization of the HIP joint comprised tensile, Charpy impact and creep testing. For tensile testing round specimens with diameter 2 mm a gauge length 7.6 mm were used. The specimens were oriented in parallel with the height of the component. The HIP joint was located in the middle of gauge length of specimens. Tensile testing was conducted on universal testing machine Zwick Z50 equipped with high temperature furnace of company Maytec. For measurement of specimen's deformation high temperature extensometer (Maytec) with

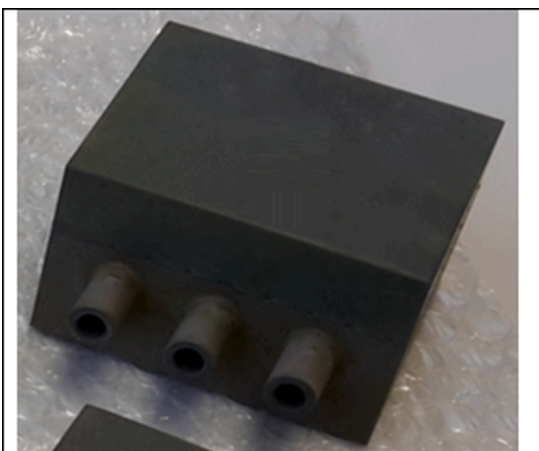


Fig. 3. First demonstration part completed.

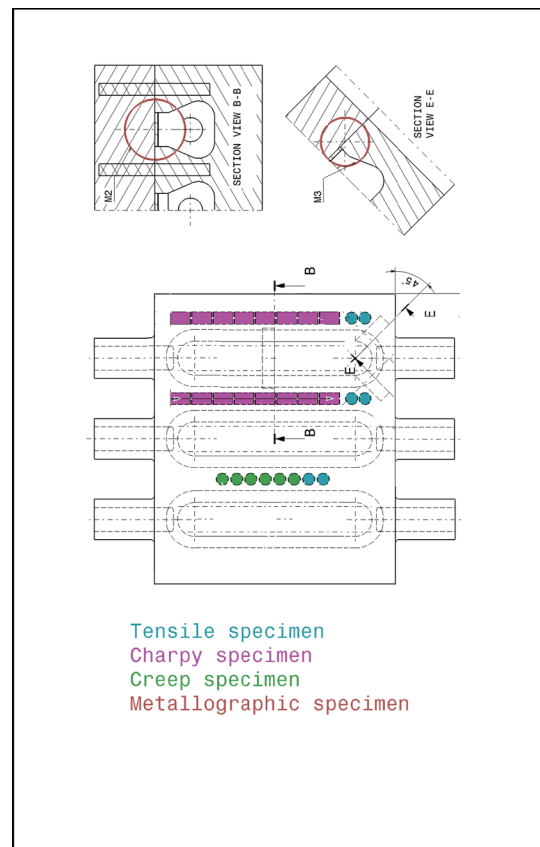


Fig. 4. Specimen extraction plan for test part qualification.

ceramics arms of gauge length 7.6 mm was used. Tensile tests were driven by displacement via cross head velocity 1.0 mm/min corresponding to the deformation rate $2.1 \cdot 10^{-3} \text{ s}^{-1}$ at the temperatures 23, 300, 400, 500 and 550 $^{\circ}\text{C}$. The one specimen per the test conditions was tested.

For Charpy impact testing, the specimens' type of KLST (Miniaturized Low Energy Charpy specimen geometry) with dimensions $3 \times 4 \times 27 \text{ mm}^3$ and V-notch (depth 1 mm, angle 60 $^{\circ}$, radius 0.1 mm) was used. Impact testing was conducted on instrumented impact tester Zwick/Roell B5113.303 with hammer capacity 15 J, velocity $3.8 \text{ m} \cdot \text{s}^{-1}$ and the span of anvils 22 mm. Impact testing was performed in the temperature range from -125 to $+300 \text{ }^{\circ}\text{C}$. The V-notch tip of KLST specimens was located at the interface of the HIP joint. In total, fifteen KLST specimens with the HIP joint were tested.

For purposes of comparison with the properties of P92 steel, tensile and KLST specimens from the cover and substrate plate of the component were fabricated. The same geometries of tensile and KLST specimens as described above were used. Those specimens were longitudinally oriented in parallel with the base plane of the component. Testing of these specimens was carried out at the same conditions as described in the case of specimens with the HIP joint. In total, seven tensile and nine KLST specimens were tested for each plate.

Creep testing of the HIP joint was done using the same specimen's geometry and orientation as for tensile test specimens with the HIP joint. Creep tests were carried out on the lever arm creep machine of IPM design in the regime of constant load in the argon (Ar 4.8) atmosphere at 550 $^{\circ}\text{C}$. The level of constant initial stress loading varied in 20 MPa steps from 320 MPa to 220 MPa.

Metallography and hardness measurement

The results of metallographic observation by light microscopy (LM)

are shown in Fig. 5 (one upper edge of the channel including the transition from substrate- to the cover plate including the Cold Spray deposited / MPA-material), Fig. 6 (a detail view from Fig. 5) and Fig. 7 (same as Fig. 6 but after etching). Note that for all images the cover plate is located in the upper part of the image. A very good quality of the HIP joint was observed. No significant pores or discontinuities at the interface of the HIP joint were detected by light microscopy up to the magnification 1000x.

However, the weld line marking the connection of cover and substrate plates is still visible which suggests that the plates are firmly joined with only limited grain growth through the HIP interface. The microstructure of the cover plate is formed by tempered martensitic microstructure with the average grain size around 15 μm, Fig. 7. The micro-structure of the substrate plate (with machined structure of cooling channels) is also formed by tempered martensite with larger average grain size of 70 μm, Fig. 7.

Different grain size of cover and substrate plate is a consequence of their different heat treatment history. At the beginning of the fabrication process the microstructures (grain sizes) of the plates were identical. During fabrication process of the demonstration component, before the step of deposition of Cold Spray layer, the substrate plate had been affected by the annealing treatment which caused grain growth. Afterwards, during the process of joining of the cover plate both plates had undergone common HIP treatment and following quenching and tempering.

The Cold Spray deposited layer (MPA) contains noticeable porosity. This issue will be addressed in the following production campaigns by optimization of parameters and powder specifications. The adhesion of MPA layer to the substrate plate is lower than to the upper cover plate. The weakest adhesion and the largest discontinuities between the MPA and substrate plate were observed in the transition radius/curved part of the substrate plate-MPA interface having a size up to 110 μm (Fig. 6).

The SEM observations confirmed the results of light microscopy observation. The HIP joint is firmly connected with visible weld line between the plates. The only partial grain growth through the HIP interface was observed as shown in Fig. 8. By means of SEM, no severe discontinuities were observed at the joint interface except for local and random presence of micro-sized pores with approximate size 0.2–0.3 μm at the weld line at high magnification of 20–50 kx, see Fig. 9. The results of line hardness measurement across the HIP interfaces are given in Fig. 10. Hardness testing revealed a higher hardness of the substrate plate with the average value 247 ± 3 HV1 in comparison to cover plate with the average value of 233 ± 2 HV1.

Slightly higher hardness of the substrate plate with its different grain size compared to the cover plate is the most probably connected with different heat treatment history of the plates. The transition of hardness values across the joint took place at the distance of approximately 0.8 mm determining the width of the zone of HIP joint interface between the

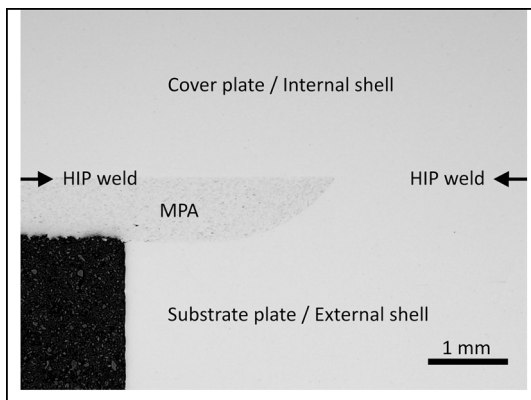


Fig. 5. Metallographic sample, non-etched state, light microscopy.

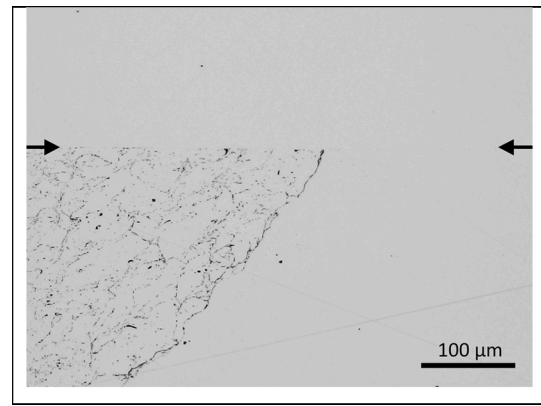


Fig. 6. Detail of the HIP joint, the intersection of plates and MPA, non-etched state, light microscopy.

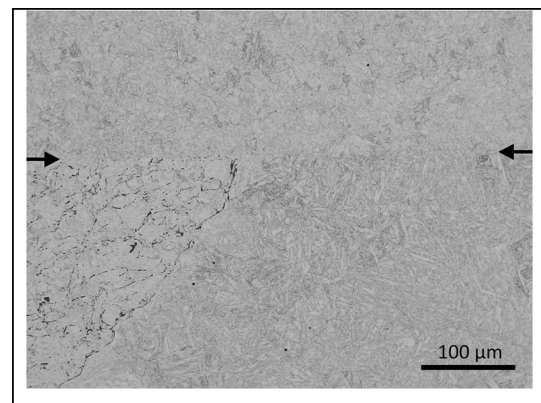


Fig. 7. Detail of the HIP joint, the intersection of plates and MPA, etched state, light microscopy.

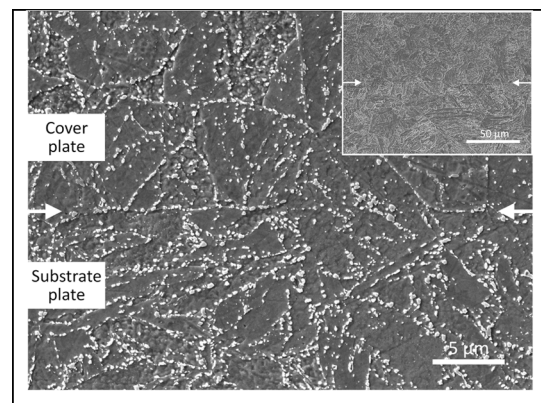


Fig. 8. Metallographic sample, HIP joint, etched state, SEM.

plates. The transition of hardness values across the interface is continuous suggesting a smooth transition of mechanical properties across it, which could imply successful joining process of the HIP treatment. The Cold Spray/MPA deposited layer has a comparable hardness level as substrate plate with the average value 250 ± 1 HV1.

Tensile testing

Tensile data of the HIP joint, substrate and cover plate are given in Table 1 and Fig. 11, Fig. 12, and Fig. 13. The HIP joint showed very similar tensile strength values and their trend over the range of test

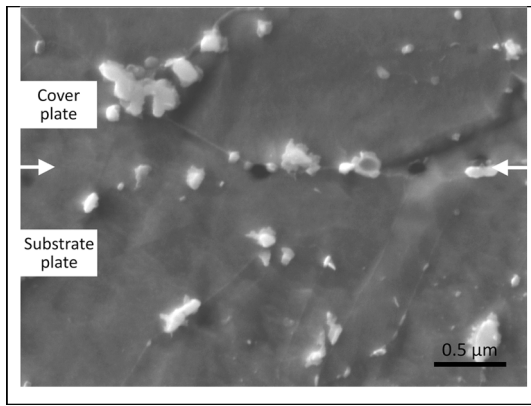


Fig. 9. Metallographic sample, HIP joint, etched state, SEM.

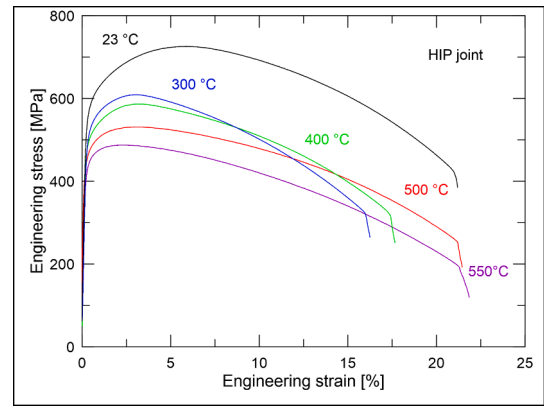


Fig. 11. Tensile curves engineering stress–strain of the HIP joint.

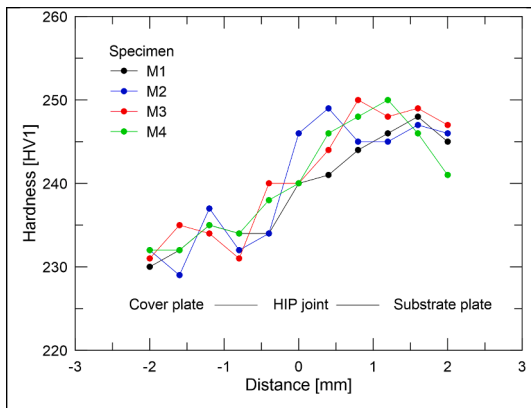


Fig. 10. Hardness across the HIP joint.

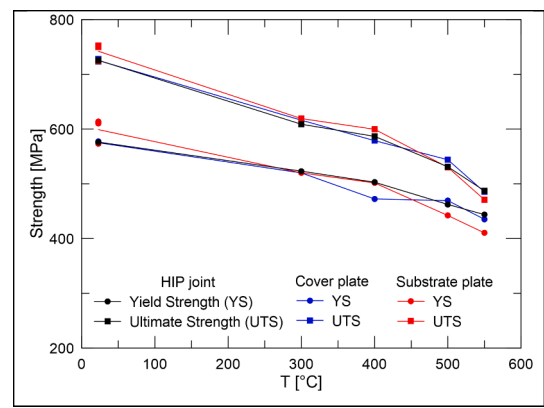


Fig. 12. Strength properties of the HIP joint in comparison with cover and substrate plate.

Table 1
Tensile test data of the HIP joint including the data of cover and substrate plate at 23 °C.

T [°C]	YS [MPa]	UTS [MPa]	A _g [%]	A [%]	Z [%]
HIP joint					
23	576	726	5.3	20.6	73.9
300	523	609	2.7	15.8	74.1
400	554	589	2.3	16.9	72.1
500	462	531	2.8	21.1	76.4
550	444	487	2.0	21.6	81.9
Cover plate					
23	575	725	7.5	25.3	74.9
	±2	±3	±0.3	±0.3	±0.1
Substrate plate					
23	599	742	6.9	24.3	73.9
	±22	±16	±0.4	±1.0	±0.9

temperatures as cover and substrate plates of the component, Fig. 12. At room temperature testing the plates pointed higher strength and lower deformation characteristics of substrate plate. The average yield and ultimate strength of substrate plate was about 24 MPa and 17 MPa higher than of cover plate, respectively. At higher temperatures with the one specimen tested, both plates show comparable values of strength and deformation characteristics. However, it's not possible to consider the scatter of test results as the only one specimen was tested at the same test conditions.

Regarding deformation properties, the average values of elongation at maximum force (A_g) and elongation (A) of substrate plate are slightly lower than of cover plate. The values of reduction of area achieved very similar values around 74–75 % for the HIP joint and both plates of basic

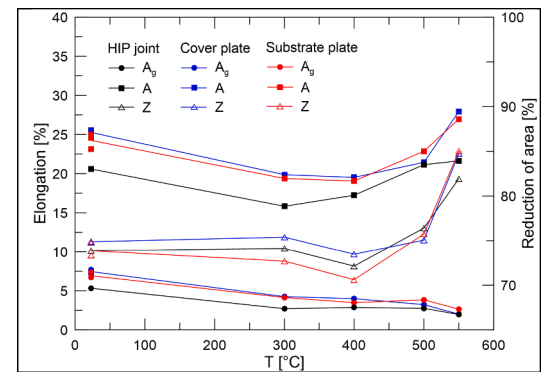


Fig. 13. Elongation of the HIP joint in comparison with cover and substrate plate.

materials. Gauge length of tensile specimens with the joint was formed from the half from cover and substrate plate between which the HIP joint was located. Due to different tensile strength properties of the plates the specimens with the joint provided non-uniform deformation along gauge length which was concentrated mainly in the one half of gauge length in material with lower yield strength. Non-proportional deformation of gauge length of the joint specimens then resulted in its limited extensions and consequently in lower elongation values both A and A_g than for basic material of cover or substrate plate. At elevated temperatures of 500 and 550 °C, the localization of fracture was shifted to the substrate plate as it provided lower tensile strength properties than cover plate. Note that different temperature dependence of tensile

strength properties of basic material was caused by different grain microstructure of the plates. In contrast to elongation, no significant differences in data of reduction of area between the HIP joint, cover and substrate plate were obtained. Therefore, non-uniform deformation of the gauge length of the specimens with the HIP joint had the only effect of decrease of elongation values. Fracture of tensile specimens was observed in the part of gauge length of material with lower yield and ultimate strength properties at test temperature i.e., the part of gauge length of cover plate material at the room temperature. These two objectives suggest that tensile elongation results of the specimens with the HIP joint are mostly affected by the connection of two plates of basic material with different microstructures than by the effect of the HIP joint which indeed indicates very good cohesion property of the connection.

Tensile test results of the HIP joint of demonstration component are also quite close to basic material of the P92 steel according to the results of Penalba et al. [22] and Barbadikar et al. [23]. In close comparison the HIP joint yields about 20–40 MPa lower yield and tensile strength than of conventional material at comparable strain rate i.e. $2.1 \cdot 10^{-3} \text{ s}^{-1}$ [23]. The elongation at maximal force and total elongation of the HIP joint are lower in comparison with the conventional P92 steel with similar difference as obtained in our study.

Charpy impact testing

The V-notch of KLST specimens was located at the interface of the joint as declared in Fig. 14. The correct location of the notch of impact specimens directly at the joint interface is an important factor for a reliable assessment of the joint property. The localization of fracture of the HIP specimen containing the HIP joint was therefore directly at the HIP interface. The results of impact testing specimens are given in Fig. 15. The specimens with the joint achieved Upper Shelf Energy (USE) 8.1 J and Ductile-to-Brittle Transition Temperature (DBTT) -69C° . At the temperature of 300C° the HIP joint still showed a very high impact energy of 7.38 J. The results of impact testing of substrate (base) and cover plate are also shown in Fig. 15. Fracture behavior of the plates was quite different having for substrate plate transition temperature -38C° and for cover plate much lower -85C° . The DBTT of the HIP joint -69C° was located between the DBTTs of the plates. A similar relation was obtained for USE as the substrate plate showed a lower value of 8.02 J than cover plate with 8.52 J. The comparison of DBTT and USE of base and cover plate and the HIP joint suggested that the joint was able to transfer different fracture behavior of the plates caused by their different grain size. Lower DBTT and USE of the substrate than of the cover plate was probably a result of softening heat treatment applied to the substrate plate before Cold Spray deposition in order to improve the adhesion of metal particles. Regarding relation of microstructural and fracture properties, higher hardness and higher grain size of substrate to

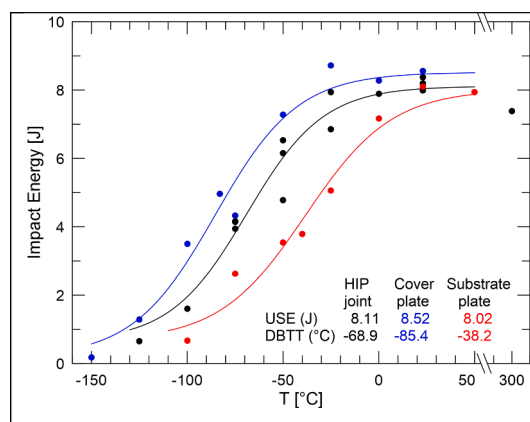


Fig. 15. Temperature dependence of impact energies of the HIP joint compared to cover and substrate plate.

cover plate corresponds to lower level of USE and DBTT of substrate plate obtained by impact testing. Similar relation between microstructural and mechanical properties had been obtained for the plates of the Eurofer97 steel with different thickness 14 and 25 mm [24].

Creep testing

The results of creep testing are shown in Table 2 and Fig. 16. Total creep test time of all six creep tests performed achieved 3789 h. The test of the specimen loaded to 220 MPa was interrupted after passing minimum creep rate at the test time 2637.4 h and creep strain 0.041. The time to fracture of this specimen, was then estimated based on the creep strain of other specimens at corresponding creep time and their time of fracture as 4550 h. Creep testing was conducted on the same specimen geometry and with the same localization of the HIP joint in the middle of gauge length as for tensile specimens. The fracture of creep specimens was located in the substrate material which is connected with lower yield strength of substrate plate than of cover plate at the test temperature of 550C° . The results of creep testing obtained are compared to selected data of Kimura et al [25]. The point of the specimen loaded to 220 MPa with the estimated time to fracture (the symbol of empty circle) is depicted in Fig. 16. Comparison of the trend of data of the HIP joint and conventional P92 steel reveals very good agreement and the slopes of the fitted curves creep stress vs. time to rupture are very close.

Conclusions to the results of destructive examination

The results of destructive examination of the HIP joint as structural weld of demonstration component provided a satisfactory level of microstructural and mechanical properties. The HIP joint did not show discontinuities, only the presence of micro-sized pores of size $0.2\text{--}0.3\ \mu\text{m}$ could be observed. The HIP joint achieved similar tensile strength properties as the substrate and cover plate. Elongation at maximum force and total elongation of the HIP joint is lower than conventional material of the P92 steel due to non-uniform deformation of the gauge length of specimens and it's not limiting for structural integrity issue of

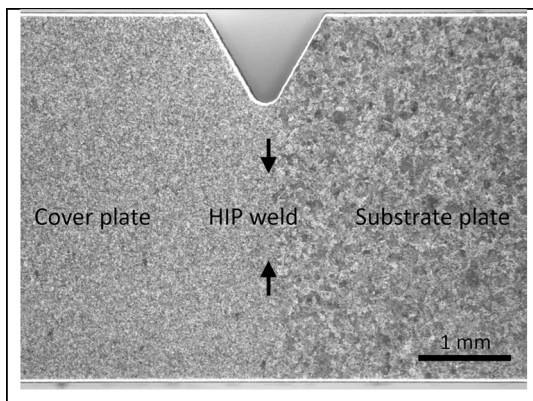


Fig. 14. Location of the V-notch of KLST specimen within the HIP joint, before testing.

Table 2
Creep Test data of the HIP joint at 550C° .

Initial Stress [MPa]	Time to fracture [h]	Creep strain [-]
320	7.0	0.143
300	19.3	0.157
280	63.6	0.169
260	203.4	0.169
240	858.4	0.171
220	*2637.4	*0.041

* Interrupted after passing minimum creep rate

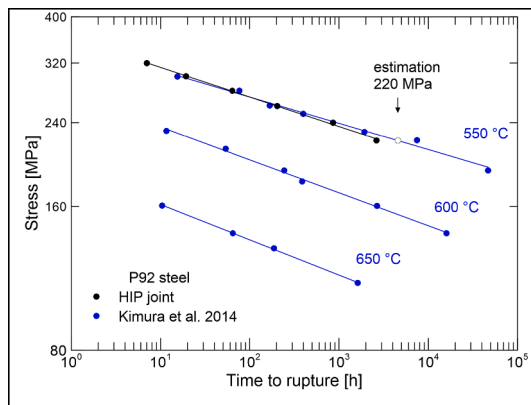


Fig. 16. Creep strength of the HIP joint of the component No. 1 in comparison with the data of Kimura et al., [25].

the component. The transition curve of the impact energy of the HIP joint lies between the transition curve of cover and substrate plate confirming its high level of Charpy impact properties. At high temperature 550 °C the creep performance of the HIP joint is found to be very similar to conventional steel, too. Based on the results of destructive examination obtained the proof of concept of applied manufacturing technology of a planar demonstration component can be derived.

Discussion of the HIP treatment parameters

Hot Isostatic Pressing (HIP) is a diffusion-based process and belongs to solid-state bonding methods of firm joining of metallic materials. Diffusion joining process requires suitable surface preparation route and joining conditions which have to be prescribed by relatively large set of parameters and was subject of several studies [26–28]. In principle, a high surface quality preparation, cleanliness and maximal contact area of surfaces are required to provide basic prerequisite for successful joining process. The most often the parts are therefore joined surface to surface in a container, which is evacuated and sealed. The bonding process is realized in a hot isostatic press under inert atmosphere and it's driven by the process parameters – pressure, temperature and time. To create diffusion joint of surfaces, a diffusion bond zone at the interface of the surfaces has to be created. Parameters which promote diffusion through the interface of surfaces and thus diffusion bond zone growth are temperature and time. Based on the diffusion theory, the contribution of temperature is much stronger over that of time [26]. The applied HIP pressure should provide firm and maximal surface connections at the interface of surfaces. Typical HIP process parameters are temperatures about 70 % of the melting point and highest possible pressure. HIP joint quality is usually evaluated by Charpy impact testing as it provides conservative assessment of cohesion properties of the connection [29].

For the Eurofer97 steel, successful joining process regarding Charpy impact properties is possible to achieve with the HIP parameters 25 MPa/1050 °C/2h [27]. However, in case of deteriorated surface quality in terms of roughness or chipping a higher HIP pressure of 100 MPa is needed. On the other hand, the contamination of joined surfaces by air oxidation can be eliminated by increased temperature to 1150 °C [27]. This temperature was also found to suppress contamination of joined surfaces caused by milling with coolant when cleaned with isopropanol which is relevant for production routes in typical industrial environments. The other study showed that the HIP treatment with parameters 150 MPa/1100 °C/2h led to the high toughness of the joint of F82H steel [29]. The key points to achieve high quality joint connection apart from those HIP parameters were identified to be a suitable final surface finishing and control of surface oxidation in the preparation step.

In our study, the main structural joint of the demonstration component was created with the HIP process parameters 140 MPa/1050 °C/

1.5 h. The applied set of HIP parameters led to good quality of the HIP joint which provided high level of mechanical properties on comparable level as the basic material. The HIP pressure of 140 MPa was used to promote sufficient surface connection of the component with planar dimensions $60 \times 72 \text{ mm}^2$. The higher pressure was chosen to suppress any possible deviation from the prescribed planarity of the surfaces and the quality of surface preparation. Both can be expected to be higher with increasing component dimensions than for laboratory size specimen/component. The temperature 1050 °C corresponding to the austenitization temperature of basic material of the P92 steel was applied for 90 min. This combination of temperature and time is rather lower than used in other studies but was still sufficient to achieve appropriate diffusion connection. Nevertheless, the presence of weld line at the joint (recognizable weld interface of the plates) indicates only limited grain growth over the interface which can be further eliminated by increased HIP temperature, e.g. 1150 °C.

Approach for demonstration of the Cold Spray based process for non-planar components

The fabrication of fully relevant First Wall shell geometries requires also the realization of non-planar surface contours. This issue has also been addressed in the 2021 and 2022 work program by out of pile experiments. The scope of these test series was to demonstrate the Cold Spray metal powder deposition with the MPA-technology for a spherical surface (Fig. 1, step 4). The specifications applied during the experiment were: a curvature radius of 200 mm (deposition surface dimensions of the test part was $\sim 150 \times 150 \text{ mm}^2$, meandering channels in relevant cross sections identically to the geometry of the planar demonstrator, Fig. 17). After deposition, the part was cut to investigate the adhesion and the transition of the deposited material on top of the substrate. The appearance has been compared to the corresponding planar fabrication experiment performed in 2020/2021. The deposited layers did not show significant differences in terms of density and adhesion (see Fig. 18, non-planar surface before HIP and compare to adhesion of MPA material after HIP in Fig. 6). Therefore, it was demonstrated that the layer of metal powder applied by deposition is also suitable to provide a leak tight membrane on top of the machined grooves for the HIP process to join the cover plate (compare to step 6 in Fig. 1). In addition to the part tested by destructive examination, another identical part exists and has been already deposited by the Cold Spray process using the identified parameters. This component will be completed by applying the



Fig. 17. Demonstration part with spherical surface contour, sections for examination.

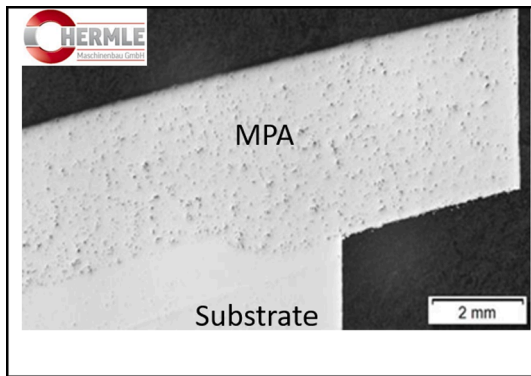


Fig. 18. Cold Spray Deposition (MPA) of curved Surface with radius of 200 mm (before thermal treatment).

fabrication steps 5 – 9 of Fig. 1 in 2023. A destructive examination campaign will follow in 2023/2024 corresponding to the qualification procedure described in [15].

Options for ODS fabrication

Oxide Dispersion Strengthened (ODS) materials are used in specific technological fields where highest requirements exist concerning operating temperatures, e.g. in manufacturing of turbine blades, heat exchanger devices and nuclear applications. Dedicated material development activities have been launched e.g. in the US, in the EU and Japan, [30–33].

Producing the plasma facing highly heat and neutron loaded Breeding Blanket components (including adjacent internal structures) from ODS-EUROFER will provide advantages compared to a pure EUROFER 97 made First Wall component [34], namely:

- the nano-sized ODS particles provide a trapping effect to hydrogen and helium. The latter is generated due to transmutation effects during neutron irradiation resulting in formation of Helium bubbles that significantly degenerate the material properties if a critical size is reached.
- compared to conventional steels, ODS steels provide improved creep resistance and tensile ductility under irradiation.
- an increased limit of the envisaged operation temperature is possible e.g. in the order of ~ 100 K demonstrated with an experimental mock up [34]. Thus, a higher dpa rate limit can be achieved compared to conventional materials like EUROFER 97. Also longer operating times of components could be reached as well as a higher efficiency of the machine.

As mentioned in chapter 2, the low temperature direct energy deposition Additive Manufacturing technology of MPA/Cold Spray metal powder deposition combined with machining and temporary filling of grooves with water soluble granulate for production of cavities provided by the supplier Hermle provides interesting possibilities for combination with already developed fabrication and HIP joining processes of ODS steel materials. This topic is planned to be addressed starting from early 2023 involving the wide experience in terms of production and testing of ODS EUROFER components of KIT IAM to exploit synergies production of hot cross rolled ODS plates joined by HIP welding and the Cold Spray metal powder deposition based First Wall fabrication process.

Based on possible combinations of the fabrication procedures Fig. 1 and [34] four concepts are presently defined which could be addressed for production as mock ups to demonstrate the feasibility and for preliminary qualification and testing purpose (see Fig. 19):

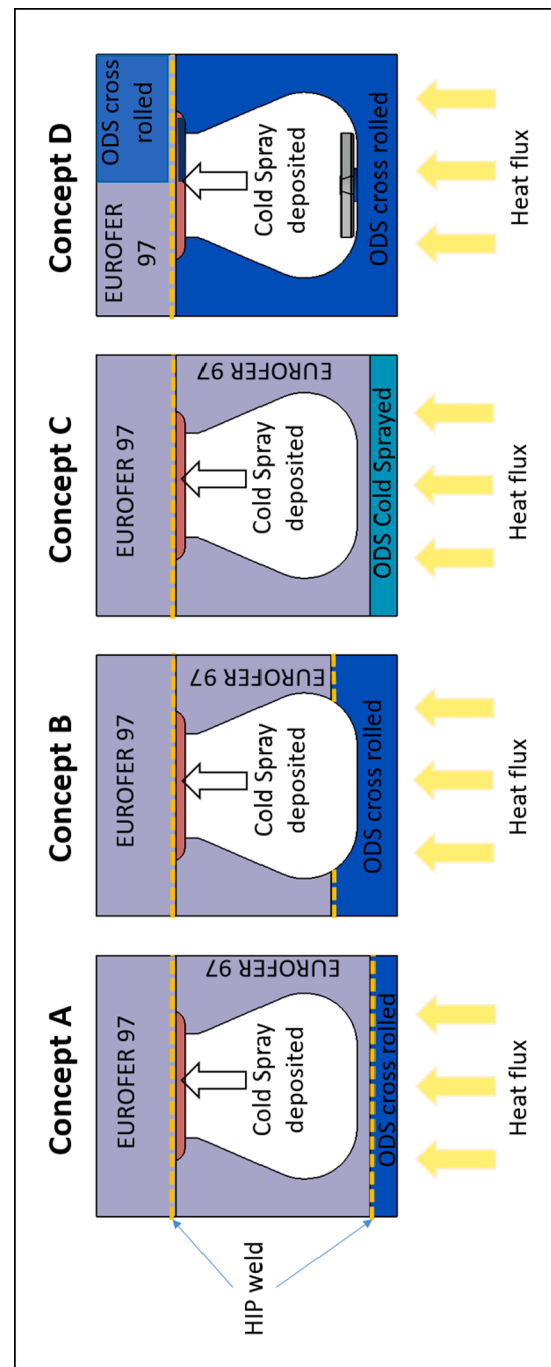


Fig. 19. Concepts for combination of hot cross rolled ODS EUROFER plate technology with Cold Spray + HIP First Wall fabrication process.

- Concept A is a direct combination of covering a First Wall surface by HIP-ping of a thin and solid layer of ODS (successfully demonstrated and tested, [34]) onto a First Wall produced by the Cold Spray based First Wall fabrication process [15].
- Concept B demonstrates a First Wall fabricated with the Cold Spray based process where a Substrate plate is used which consists of two solid plates HIP-ped together where the plasma facing side is made from ODS EUROFER and the inner side is EUROFER 97. The channels are machined into the ODS material as already demonstrated in [34].
- Concept C is an approach to directly deposit ODS EUROFER on the First Wall surface by Cold Spray metal powder deposition.
- Concept D is related to the Cold Spray deposition based First Wall manufacturing process where a substrate plate fully made from hot

cross rolled ODS EUROFER is used. On the channels bottom heat flux facing side the surface can optionally be equipped with so-called semi-detached ribs for turbulence promotion purpose, fabrication and installation according to [15], geometry parameters according to [10,11]. The cover plate is made from conventional EUROFER 97, but as alternative also ODS EUROFER powder could be used for the Cold Spray process to establish the pressure seal barrier for to join the cover plate. In case also ODS EUROFER can be used as material for the cover plate, thus a First Wall fully built from ODS EUROFER could be produced. The problem of fusion welding for connection of such devices to surrounding components can be circumvented by using the existing option to deposit graded material layers by the Cold Spray/MPA technology of Hermle (from 100 % ODS material towards 100 % conventional material) to generate welding connection studs onto the ODS shells.

Presently the concepts A) – D) using ODS EUROFER material shown in Fig. 19 are planned to be demonstrated in plane configuration firstly. As mid-term goal further options can be addressed for generation of 3D-shell geometries corresponding to the progress achieved in terms of the application of the Cold Spray based First Wall fabrication process in non-planar configuration and the achievements in terms of ODS hot cross rolling of semi-finished plates.

However the plane configuration itself in medium dimensions can already provide a basis for technology spin offs: e.g. towards plane receiver panels elements for energy production with Concentrated Solar Power (CSP). Here the possibilities of the increased operation temperatures of the structure using ODS material for monolithic devices with complex internal cooling channel structures based on HIP joints without any fusion welding remaining in the final product offers new promising possibilities.

Outlook on the next development steps

The scope until end of EUROFUSION FP9 [9] in terms of development and demonstration of the First Wall manufacturing technologies involving Additive Manufacturing described in this paper is to demonstrate proof of concept (Technology Readiness Level 3) for the integral Cold Spray based fabrication process. This goal is now achieved for the first small scale planar demonstration part. Presently also the same demonstration and qualification routine is addressed to new series of demonstration parts: planar components corresponding to the specifications of the part described in this paper are planned to be built and qualified in late 2022/early 2023. However, the dimensions of the 2nd series of planar demonstrators are scaled of by a factor of 10 in terms of the heat flux surface. Larger demonstration parts towards fusion relevant dimensions using the maximum size available in terms of industrial equipment (~0.5 m² heat flux facing surface in terms of Cold Spray metal powder deposition/MPA) will be envisaged after 2024. Also in terms of the non-planar mock ups the achievement of TRL 3 is envisaged before the end of FP9.

Another topic to be investigated more deeply now after proof of concept of the First Wall manufacturing process has been reached is the metal powder properties used for the Cold Spray deposition. Impurities (mainly O₂) as well as the powder grain shape, powder grain size/distribution and the microstructure of the powder needs to be specified in detail to reach an optimum in terms of ductility and strength of the deposited material. Also necessity of the thermal treatment of the substrate plate before Cold Spray deposition will be examined in dedicated experiments.

In parallel, the investigations concerning options of fabrication of First Wall devices with ODS materials will be initiated in 2023 in out of pile experiments using the Cold Spray based process configuration. The technological developments will be also studied in terms of spin-off options, e.g. towards the fabrication of plate receivers for Concentrated Solar Power (CSP) and comparable high heat flux devices.

Conclusion

Technology Readiness Level TRL 3 has been demonstrated for the Cold Spray based hybrid First Wall manufacturing concept by mechanical qualification. Profound destructive examination of the HIP weld as main structural joint of the component showed mechanical and fracture properties on the level of basic material of P92 steel. The applied process parameters in term of component preparation steps and HIP treatment parameters will provide the basis for further medium scale and non-planar demonstrators.

CRedit authorship contribution statement

Heiko Neuberger: Conceptualization, Methodology, Investigation, Writing – original draft, Writing – review & editing, Visualization. **Francisco Hernandez:** Writing – review & editing. **Michael Rieth:** Investigation, Writing – review & editing. **Carsten Bonnekoh:** Investigation, Writing – review & editing. **Ludek Stratil:** Conceptualization, Methodology, Investigation, Writing – original draft, Visualization. **Ivo Dlouhy:** Investigation, Writing – review & editing. **Petr Dymacek:** Investigation, Writing – review & editing. **Oliver Müller:** Conceptualization, Methodology, Investigation. **Lucas Adler:** Conceptualization, Methodology, Investigation. **Ulrich Kunert:** Investigation.

Declaration of Competing Interest

The authors declare that they have no known competing financial interests or personal relationships that could have appeared to influence the work reported in this paper.

Data availability

The data that has been used is confidential.

Acknowledgment

This work has been carried out within the framework of the EUROfusion Consortium, funded by the European Union via the Euratom Research and Training Programme (Grant Agreement No 101052200 - EUROfusion). Views and opinions expressed are however those of the author(s) only and do not necessarily reflect those of the European Union or the European Commission. Neither the European Union nor the European Commission can be held responsible for them.

Next, the support of the project no. MSM100411601 within the Programme for research and mobility support of starting researchers of Czech Academy of Sciences is greatly appreciated.

References

- [1] H. Neuberger, et al., KIT induced activities to support fabrication, assembly and qualification of technology for the HCPB-TBM, *Fusion Eng. Des.* 86 (9–11) (2011) 2039–2042, <https://doi.org/10.1016/j.fusengdes.2011.03.016>.
- [2] M. Rieth et al., Cost effective fabrication of a fail-safe first wall, DOI: 10.5445/IR/230081118.
- [3] H. Neuberger, et al., Overview on ITER and DEMO blanket fabrication activities of the KIT INR and related frameworks, *Fusion Eng. Des.* 96–97 (October 2015) 315–318, <https://doi.org/10.1016/j.fusengdes.2015.06.174>.
- [4] L. Forest, et al., Test blanket modules (ITER) and breeding blanket (DEMO): History of major fabrication technologies development of HCLL and HCPB and status, *Fusion Eng. Des.* 154 (May 2020), 111493, <https://doi.org/10.1016/j.fusengdes.2020.111493>.
- [5] L. Forest et al., The European ITER Test Blanket Modules: Fabrication R&D progress for HCLL and HCPB Fusion Engineering and Design, Volume 136, Part B, November 2018, Pages 1408–1416, <https://doi.org/10.1016/j.fusengdes.2018.05.026>.
- [6] F. Hernandez, et al., A new HCPB breeding blanket for the EU DEMO: Evolution, rationale and preliminary performances, *Fusion Eng. Des.* 124 (November 2017) 882–886, <https://doi.org/10.1016/j.fusengdes.2017.02.008>.
- [7] F. Hernandez et al., Advancements in the Helium-Cooled Pebble Bed Breeding Blanket for the EU DEMO: Holistic Design Approach and Lessons Learned, *Fusion Science and Technology*, Volume 75, 2019 - Issue 5: Selected papers from the 23rd

- Topical Meeting on the Technology of Fusion Energy—Licensing, New Facilities, and Safety, Pages 352-364, <https://doi.org/10.1080/15361055.2019.1607695>.
- [8] L.V. Boccaccini, et al., Status of maturation of critical technologies and systems design: Breeding Blanket, *Fusion Eng. Des.* 179 (2022), 113116, <https://doi.org/10.1016/j.fusengdes.2022.113116>.
- [9] G. Federici, et al., The plan forward for EU DEMO, *Fusion Eng. Des.* 173 (2021), 112960, <https://doi.org/10.1016/j.fusengdes.2021.112960>.
- [10] Sebastian Ruck, et al., Structured Cooling Channels for Intensively Heated Blanket Components, 2021, <https://doi.org/10.5445/IR/1000085675> <https://publikationen.bibliothek.kit.edu/1000085675>.
- [11] F. Arbeiter, et al., Thermal-hydraulics of helium cooled FW channels and scoping investigations on performance improvement by application of ribs and mixing devices, *Fusion Eng. Des.* 109–111 (B) (2021), <https://doi.org/10.1016/j.fusengdes.2016.01.008>.
- [12] P. Grandl, Additive Manufacturing of Liquid Rocket Engine Combustion Devices: A Summary of Process Developments and Hot-Fire Testing Results, 54th AIAA/SAE/ASEE Joint Propulsion Conference 2018, AIAA - 2018 - 4625.
- [13] H. Neuberger, et al., Selective Laser Sintering as manufacturing process for the realization of complex nuclear fusion and high heat flux components, *Fusion Sci. Technol.* 72 (2017), <https://doi.org/10.1080/15361055.2017.1350521>. - Issue 4: Selected papers from the Twenty-Second Topical Meeting on the Technology of Fusion Energy—Part 2.
- [14] C. Koehly, et al., Fabrication of thin-walled fusion blanket components like flow channel inserts by selective laser melting, *Fusion Eng. Des.* 143 (June 2019) 171–179, <https://doi.org/10.1016/j.fusengdes.2019.03.184>.
- [15] H. Neuberger, et al., Advances in Additive Manufacturing of fusion materials, *Fusion Eng. Des.* 167 (June 2021), 112309, <https://doi.org/10.1016/j.fusengdes.2021.112309>.
- [16] S. Bonk, et al., Additive manufacturing technologies for EUROFER97 components, *J. Nucl. Mater.* 548 (May 2021), 152859, <https://doi.org/10.1016/j.jnucmat.2021.152859>.
- [17] S. Bonk, et al., Microstructural features in additively manufactured EUROFER97 components, *Fusion Eng. Des.* 173 (December 2021), 112813, <https://doi.org/10.1016/j.fusengdes.2021.112813>.
- [18] Karlsruher Institut für Technologie, Mehrwandiges Rohrbauteil und Herstellungsverfahren dafür, DE 10 2016 115 335 A1 2018.02.22.
- [19] Karlsruher Institut für Technologie, Generative Fertigungsanlage und Verfahren zur Herstellung von Bauteilen mittels dieser generativen Fertigungsanlage, DE 10 2017 118 065 A1 2019.02.14.
- [20] Karlsruher Institut für Technologie, Verfahren zur Herstellung von Rohren mit topographischen Innenstrukturen, DE 10 2021 106 305 A1 2022.09.22.
- [21] F. Tavassoli, Eurofer Steel, Development to Full Code Qualification, 6th International Conference on Creep, Fatigue and Creep-Fatigue Interaction [CF-6], *Procedia Engineering* 55 (2013) 300 - 308.
- [22] F. Peñalba, et al., Effect of Temperature on Mechanical Properties of 9%Cr Ferritic Steel, *ISIJ Inter.* 56 (2016) 1662–1667, <https://doi.org/10.2355/isijinternational.ISIJINT-2016-097>.
- [23] D.R. Barbadikar, et al., Investigation on mechanical properties of P92 steel using ball indentation technique, *Mat. Sci. Eng. A* 624 (2015) 92–101, <https://doi.org/10.1016/j.msea.2014.11.075>.
- [24] L. Stratil, H. Hadraba, J. Bursik, I. Dlouhy, Comparison of microstructural properties and Charpy impact behaviour between different plates of the Eurofer97 steel and effect of isothermal ageing, *J. Nucl. Mater.* 416 (2011) 311 317, <https://doi.org/10.1016/j.jnucmat.2011.06.018>.
- [25] K. Kimura, K. Sawada, H. Kushima, Creep deformation, rupture strength, and rupture ductility of Grades T/P92 Steels. In Proceedings of the ASME Symposium on Elevated Temperature Application of Materials for Fossil, Nuclear, and Petrochemical Industries, ASME, 2014, ETAM2014-1026, pp. 193-201, <https://doi.org/10.1115/ETAM2014-1026>.
- [26] M. Rieth, et al., Technological Processes for Steel Applications in Nuclear Fusion, *App. Sci.* 11 (2021) 11653, <https://doi.org/10.3390/app112411653>.
- [27] M. Rieth, et al., Diffusion weld study for Test Blanket Module fabrication, *Fusion Eng. Des.* 84 (2009) 1602–1605, <https://doi.org/10.1016/j.fusengdes.2009.02.006>.
- [28] T. Hirose, et al., Fabrication of first wall component of ITER test blanket module by HIPping reduced activation ferritic/martensitic steel, *Adv. Technol. Mater. Mater. Process. J.* 13 (2011) 34–38. <https://jopss.jaea.go.jp/search/servlet/search?5030018&language=1>.
- [29] T. Hirose, et al., Joining technologies of reduced activation ferritic/martensitic steel for blanket fabrication, *Fusion Eng. Des.* 81 (2006) 645–1561, <https://doi.org/10.1016/j.fusengdes.2005.07.015>.
- [30] M. Lenling, et al., Manufacturing Oxide Dispersion Strengthened (ODS) Steel Fuel Cladding Tubes using the Cold Spray Process, *JOM* 71 (8) (2019) 2868–2873, <https://doi.org/10.1007/s11837-019-03582-w>.
- [31] H. Yeom, et al., Cold Spray Manufacturing of Oxide-dispersion Strengthened (ODS) Steels using Gas-atomized and Ball-milled 14YWT powders, *J. Nucl. Mater.* 574 (2023), 154187, <https://doi.org/10.1016/j.jnucmat.2022.154187>.
- [32] J. Hoffmann, Ferritische ODS-Stähle - Herstellung, Umformung und Strukturanalyse. Karlsruhe: KIT Scientific Publishing, 2014. DOI: <https://doi.org/10.5445/KSP/1000037770>.
- [33] S. Ohtsuka et al., High-temperature creep properties of 9Cr-ODS tempered martensitic steel and quantitative correlation with its nanometer-scale structure, *J. Nucl. Sci. Technol.*, 2022, <https://doi.org/10.1080/00223131.2022.2096147>.
- [34] M. Rieth, et al., Impact of materials technology on the breeding blanket design – Recent progress and case studies in materials technology, *Fusion Eng. Des.* 166 (2021), 223375, <https://doi.org/10.1016/j.fusengdes.2021.112275>.